Chemical Papers (2021) 75:4697–4706
https://doi.org/10.1007/s11696-021-01684-x

ORIGINAL PAPER

A high selective "turn-on" fluorescent chemosensor for detection of Zn^{2+} in aqueous media

Juan Li[1] · Shu-Zhen Zhang[1] · Geng Guo[1] · Hao-Ran Jia[1] · Yin-Xia Sun[1]

Received: 6 February 2021 / Accepted: 26 April 2021 / Published online: 18 May 2021

Abstract

A simple Schiff base fluorescent probe (SW) composed of oxime and salicylaldehyde units was designed and synthesized. The probe has high selectivity and sensitivity for Zn^{2+} ion in mixed solvent (DMSO/H_2O, V/V = 9:1). The fluorescence has obvious redshift phenomenon and visible color change. The stoichiometric ratio of the probe to Zn^{2+} ion was confirmed to be 1:2 (mole) by ^{1}H NMR, MS analysis and job curves. And the detection limit of fluorescence response of the SW to Zn^{2+} is down to 2.53×10^{-8} mol/L. At the same time, the probe SW can be applied to the test paper detection of Zn^{2+} ions under 365 nm UV light and the detection of Zn^{2+} ions in actual water samples.

Keywords Fluorescent probe · Schiff base containing oxime · Zn^{2+} recognition · Test paper · Actual water samples

Introduction

Zinc is the second most abundant transition metal ion in the human body after iron. It plays an important role in various physiological and pathological processes, including DNA synthesis, gene expression, enzyme regulation structure and neuron signal transmission (Wang et al. 2020a, b, c, d; Zhang et al. 2021). The lack of Zn^{2+} in adults can lead to neurological disorders, Alzheimer's disease and diabetes. Lack of Zn^{2+} in children can lead to decreased immune function, diarrhea and even death (Vetriarasu et al. 2019; Liu et al. 2020a, b). In recent years, zinc ion is widely used in electroplating industry, which causes more and more serious environmental pollution. Therefore, it is very important for human health and environment to design a high selective zinc ion detection probe (Zhao et al. 2019; Yu et al. 2017b, a). Although many chemical sensors for zinc detection have been studied before, new fluorescent probes for selective detection of zinc ions in physiological pH conditions and environmental systems are still in great demand. Due to its d^{10} configuration, Zn^{2+} sensor is usually interfered by other d^{10} metal ions (such as Cd^{II} and Hg^{II}) (Anand et al. 2018; Bian et al. 2021b, a). As we all know, Schiff base fluorescent probe is a kind of metal ion probe which is relatively simple to synthesize and widely used. It has the advantages of convenient operation, simple detection method, fast detection and high sensitivity, and has attracted great attention. Because of the C = N group in its structure, its rigid structure and fluorescence are enhanced after chelating with metal ions (Patil et al. 2018; Xu et al. 2021a, b).

In this paper, we designed and synthesized a fluorescent probe SW with high selectivity and sensitivity for the detection of Zn^{2+} ions, which can be used for visual detection. The probe has the advantages of simple preparation and low cost (Wei et al. 2020; Pannipara et al. 2018). It has a strong practical value for the test paper detection of Zn^{2+} ions under 365 nm UV light and the detection of Zn^{2+} ions in actual water samples.

Experimental

Materials and methods

The O-benzylhydroxylamine (99%), 4-aminoacetophenone (99%), and salicylic aldehyde (98%) used in the experiment were purchased from Alfa Aesar. The remaining reagents and solvents are all analytical reagents and can be used without further purification. The water used in the experiment is distilled water. The X-4 microscopic melting point

✉ Yin-Xia Sun
Sun_yinxia@163.com

[1] School of Chemical and Biological Engineering, Lanzhou Jiaotong University, Lanzhou 730070, People's Republic of China

instrument produced by Beijing Tyco Instrument Limited company was used for melting point measurement, and no calibration was performed before use. German Vario EL V3.00 automatic element analyzer was used for the analysis of C, H, and N elements. ^{1}H NMR spectra were recorded in DMSO-d6 solution using Bruker AV series DRX-500 MHz nuclear magnetic resonance instrument. Fluorescence spectra were recorded using Hitachi (Japan) F-7000 fluorescence spectrophotometer. Ultraviolet–visible absorption spectrum is measured by Hitachi UV-3900 spectrometer. The B3LYP/6-31G function is used as the basis of geometric optimization, and the Gaussian 09 software program is used for DFT calculation.

By adding various metal cations in DMSO/H_2O (V/V = 9:1) medium, and the probe SW concentration was kept constant (2.0×10^{-4} mol/L). All metal cation solutions (1.0×10^{-2} mol/L) Na^+, Al^{3+}, Ba^{2+}, Ca^{2+}, Cd^{2+}, Co^{2+}, Cr^{3+}, Fe^{3+}, Mg^{2+}, Mn^{2+}, Zn^{2+}, Ni^{2+}, Pb^{2+}, Hg^{2+} and Cu^{2+} were prepared from the nitrate salts, while the Zn^{2+} solutions was prepared by $Zn(NO_3)_2$. The excitation wavelength used for fluorescence spectrometry is 368 nm, the entrance slit is 5 nm and the exit slit is 5 nm.

Synthesis of the probe SW

SW was synthesized routes shown in Scheme 1. O-benzylhydroxylamine (1.18 g, 9.0 mmol) and 4-aminoacetophenone (1.22 g, 9.0 mmol) were dissolved in anhydrous ethylalcohol (15 mL), and then 3 drops of glacial acetic acid were added to the mixed solution and refluxed at 65 °C for 6 h. The mixture solution is cooled, filtered to obtain a yellowish solid, washed with anhydrous ethanol/water (V/V = 1:4) and dried under vacuum (Sun et al. 2015; Wu et al. 2021), and obtained in 2.05 g of ({4-amino}phenyl)ethanone O-benzyl oxime as crystalline solid. Yield: 89.0%. M.p.351 ~ 352 K. Anal. Calcd. for $C_{15}H_{16}N_2O$(%): C, 74.97; H, 6.71; N, 11.66. Found (%): C, 74.68; H, 6.80; N, 11.52.

({4-amino}phenyl)ethanone O-benzyloxime (1.51 g, 6 mmol) and salicylaldehyde (0.74 g, 6 mmol) were dissolved in ethanol (15 mL), and the mixed solution was stirred at 65 ℃ for 6 h. After cooling to room temperature, vacuum distillation and filtration were carried out. The precipitate was washed with ethanol/n-hexane (V/V = 1:4). After vacuum drying, 1.37 g SW dark yellow solid product was obtained (Fig S1). Yield: 61.3%. M.p. 229 ~ 230 ℃, Anal. Calcd. for $C_{22}H_{20}N_2O_2$ (%): C, 76.72; H, 5.85; N, 8.13. Found (%): C, 76.97; H, 5.23; N, 8.25. ^{1}H NMR (500 MHz, DMSO-d_6) δ 12.96 (s, 1H), 8.99 (s, 1H), 7.78—7.72 (m, 2H), 7.68 (dd, J = 7.7, 1.8 Hz, 1H), 7.47–7.36 (m, 7H), 7.35—7.29 (m, 1H), 7.03—6.95 (m, 2H), 5.22 (s, 2H), 2.25 (s, 3H).

Results and discussion

Fluorescence recognition of Zn^{2+} by probe SW

The response of probe SW to different metal cations was studied by the fluorescence method at room temperature (Li et al. 2021a, b, c). As shown in Fig. 1a, fifteen cations (Na^+, Al^{3+}, Ba^{2+}, Ca^{2+}, Cd^{2+}, Co^{2+}, Cr^{3+}, Fe^{3+}, Mg^{2+}, Mn^{2+}, Zn^{2+}, Ni^{2+}, Pb^{2+}, Hg^{2+} and Cu^{2+}) (1.0×10^{-2} mol/L) were added to the solution of probe SW (2.0×10^{-4} mol/L) (DMSO/H_2O, V/V = 9:1), respectively. When the excitation wavelength is 368 nm, the probe SW has a weak fluorescence emission peak at 437 nm. After the addition of other metal ions, the intensity of emission peak has no obvious enhancement except Zn^{2+} ions. Furthermore, the emission peak was red-shifted from 437 to 502 nm and the intensity increased by 16 times upon addition of Zn^{2+} ions (Dong et al. 2017; Wang et al. 2020a). Under the UV lamp, the solution of 15 kinds of metal ions to be measured was added to DMSO/H_2O solution (V/V = 9:1) of SW in turn, a strong bright green fluorescence is produced only added Zn^{2+} ions, and other metal cations have basically no obvious effect (Anand et al. 2017; Pan et al. 2020a, b), the fluorescence remains unchanged or quenched (Fig. 1b). It can prove that probe SW could selectively identify Zn^{2+} ion among other metal ions to be measured. It is helpful to study the high sensitivity of probe SW to Zn^{2+} ion by anti-interference experiment (Ozdemir 2016; Sun et al. 2019). In Fig. 2, after adding Zn^{2+} ion to

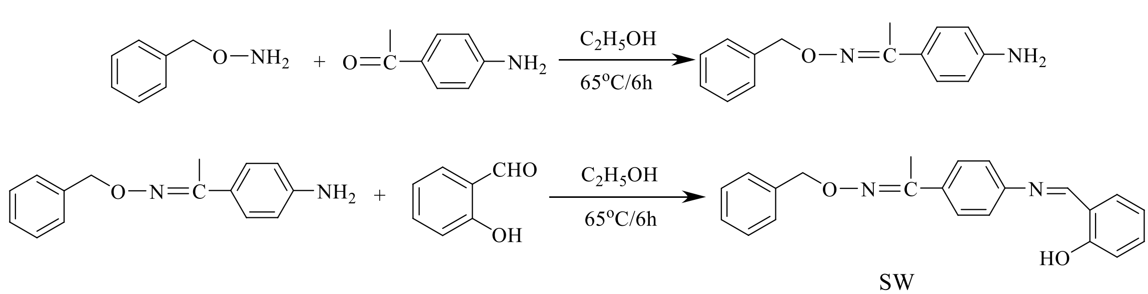

Scheme 1 Synthetic routes of SW

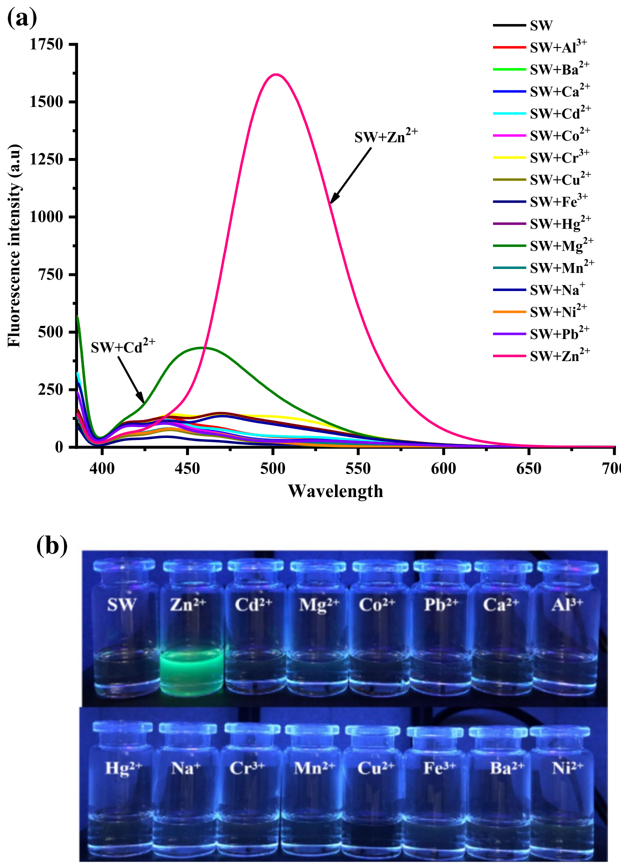

Fig. 1 **a** Fluorescence emission spectra of probe SW with various metal ions in DMSO/H_2O (v/v = 9:1) medium (λ_{ex} = 368 nm); **b** Fluorescence changes upon different cationic added to the SW solution in DMSO/H_2O (v/v = 9:1) solution under 365 nm UV lamp

probe SW solutions containing different metal ions, other metal cations had no markedly effect on the fluorescence recognition to Zn^{2+} ions except for the slight quenching of Cu^{2+} ion and Co^{2+} ion had a slight effect (Liu et al. 2020a). The results show that SW has good selectivity for Zn^{2+} ions.

In order to quantitatively evaluate the fluorescence sensing behavior of SW, we carried out fluorescence titration experiment. As shown in Fig. 3, the Zn^{2+} solution (1.0×10^{-3} mol/L) was gradually added to the probe SW solution (2.0×10^{-4} mol/L) (Upadhyay et al. 2018; Wang et al. 2021a, b), the free SW exhibited a weak emission peak at 437 nm, a new peak emission present at 507 nm and its intensity gradually increased when the concentration of Zn^{2+} ion increases continuously (Wang et al. 2017; Chang et al. 2020). When the Zn^{2+} content reaches 0.5 equivalent, the fluorescence emission intensity reaches the maximum, indicating that the optimal binding ratio of Zn^{2+} to probe SW is 1:2. Bringing the results of titration experiments into the Benesi–Hildebrand equation $\{1/(F - F_0) = 1/(F_{max} - F_0) + 1/K_d[\mathrm{C}] \times 1/(F_{max} - F_0)\}$ (Sudipa et al. 2019; Xu et al. 2021a), and the binding constant is calculated as K_a = 7.7×10^4 M^{-1} (Fig. S2a). Where, F_0, F and F_{max} are the fluorescence intensity without Zn^{2+}, the fluorescence intensity at any given Zn^{2+} concentration and the fluorescence intensity after titration saturation, respectively. The limit of detection LOD for Zn^{2+} toward SW was calculated using LOD = 3σ/slope and was found to be 2.53×10^{-8} mol/L (Fig. S2b) (Wang et al. 2020b; Purkait et al. 2019). Among them, the standard deviation σ was calculated by measuring five consecutive fluorescence intensities of probe SW, and the slope was obtained by plotting the relationship between the emission intensity of SW and the concentration of Zn^{2+} (Zhang et al. 2020; Bian et al. 2021b; Fan et al.

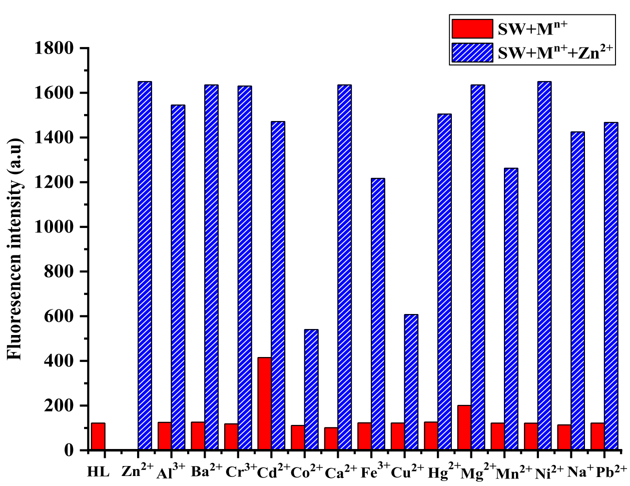

Fig. 2 Fluorescence emission spectra (λex = 368 nm) of the probe SW in the presence of Zn^{2+} and various cationic in DMSO/H_2O (v/v = 9:1) solution

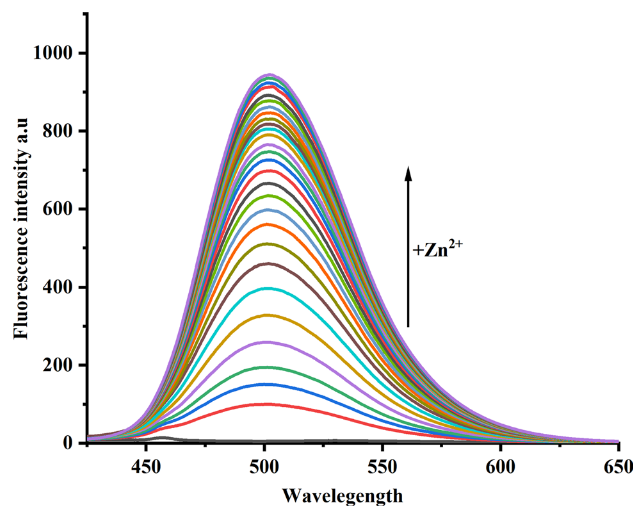

Fig. 3 Fluorescence spectra of the probe SW in DMSO/H_2O (v/v = 9:1) solution with increasing concentration of Zn^{2+} (0–0.5equiv)

2020). The calculated results are lower than the acceptable limit (7.0×10^{-6} mol/L) of WHO drinking water (Lu et al. 2020; Kang et al. 2019b). Compared with other Zn^{2+} sensors reported previously, the detection limit is lower and the sensitivity is higher (Table 1).

In order to test and verify the rapid detection performance of probe SW for Zn^{2+}, the Zn^{2+} response time experiment was carried out (Zhang et al. 2019). As shown in Fig. S3, after adding Zn^{2+}, the response time of probe SW was 3 min (Pan et al. 2020a; Li et al. 2021a). The fluorescence reversibility studied by adding Zn^{2+} and ethylenediaminetetraacetic acid (EDTA, $c=1.0\times10^{-3}$ mol/L) to SW solution. In Fig S4, when EDTA was introduced to SW and Zn^{2+} mixed solution, the fluorescence intensity at 502 nm was diminished. Then, Zn^{2+} solution was added again, and the fluorescence intensity was close to the initial fluorescence value, and the above experimental steps were repeated, and the fluorescence intensity continued to decrease and increase (Wang et al. 2021a; Mu et al. 2020). Thus, the probe SW can monitor Zn^{2+} reversibly.

UV–Vis spectroscopic studies of Zn^{2+} by probe SW

In the UV–Vis spectrum, as shown in Fig S5a, the free ligand SW exhibited a weak absorb peak at 425 nm. When Zn^{2+} ions were added to probe SW solution, a new absorption peak appeared at 458 nm, and the solution changed from colorless to yellow (Fig. S5b). At the same time, the addition of Co^{2+}, Fe^{3+} and Cu^{2+} metal ions also slightly changed the color. Therefore, UV–Vis spectrum can be used as an assistant method to detect the Zn^{2+} by this probe SW. As shown in Fig. S6, the Zn^{2+} solution (1.0×10^{-3} mol/L) was gradually added to the probe **SW** solution (2.0×10^{-4} mol/L) for UV–visible titration experiments (Wang et al. 2020c; Liu et al. 2018). With the continuous increase of Zn^{2+} concentration, a new absorption peak appears at 458 nm, while the absorption peak at 352 nm gradually decreases. At the same time, an isoabsorptive point appeared at 285 nm and until the content of Zn^{2+} solution reached 0.5 equivalents, the peaks at 458 nm and 352 nm remained unchanged (Fig. S7b). The UV–Vis spectral characteristics support the molar ratio of metal to ligand of 1:2, and the association constant $K_a=5.6\times10^4$ M^{-1} (Fig. S7a).

The detection mechanism of the probe SW for Zn^{2+}

^1H NMR titration experiment was carried out in DMSO-d_6 (Long et al. 2020). As shown in Fig. 4, with the addition of Zn^{2+} from 0 to 0.5 equivalent, the phenolic hydroxyl protons H1 ($\delta=12.87$ ppm) gradually disappeared until completely disappeared, indicating the deprotonation process of hydroxyl induced by Zn^{2+}. With the addition of Zn^{2+}, azomethine H2 (HC = N) shifts from 9.02 ppm to 8.65 ppm, which may be due to the coordination between imine-N and Zn^{2+}. In the complex SW-Zn^{2+}, the ^1H NMR titration data supports 1:2 metal–ligand ratio (Xu et al. 2020; Yu et al. 2017a). Job's plot further analyzes the coordination ratio between SW and Zn^{2+} (Fig. S8), when the mole fraction of Zn^{2+} ion is 0.345, the fluorescence intensity reaches the maximum value, showing that the binding ratio of Zn^{2+} ion to SW is 1:2 (Liu et al. 2020b; Xue et al. 2019).

As shown in Scheme 2, the fluorescence enhancement recognition mechanism of Zn^{2+} by probe SW may be mainly due to the presence of Zn^{2+} hindering the PET (light-induced electron transfer) effect of SW. Owing to the rotation of imine group (-CH = N) in free SW, there is a very weak fluorescence in SW solution. The addition of Zn^{2+} ions can coordinate with the probe SW, which inhibits the free rotation of imine group of SW molecules and produces CHEF effect (Liu et al. 2018; Zhang et al. 2018), resulting enhanced fluorescence. The mass spectrum peak of the complex appeared at 751.22 (Fig. S9), which further confirmed that the complex was consistent with the conjecture.

DFT computation

In order to further study the geometry and interaction of SW and Zn^{2+}, density functional theory (DFT) calculation was carried out. The geometry structures of SW and SW-Zn^{2+} were optimized by 6-31G/LanL2DZ basic setting program using Gausans-09 software (Feng et al. 2021; Rout et al. 2019). As shown in Fig. 5, one the Zn^{2+} ion coordinated with two ligand SW molecules. Among, the coordination atoms are hydroxyl O atoms and the imine N atoms on C = N groups of two SW molecules, respectively. The LUMO and HOMO energies of SW were −1.551 eV and −5.659 eV, respectively. The energy gap ($\Delta E=E_{LUMO}$-E_{HOMO}) was 4.108 eV, and the SW molecule was delocalized on the entire conjugated skeleton except for the oxime phenyl group. After SW coordinating with Zn^{2+}, LUMO and HOMO energies were −1.931 eV and −5.386 eV, respectively. Correspondingly, the energy gap was 3.455 eV, and the electron density was mainly delocalized on the two Schiff groups and mainly on entire salicylaldehyde and aminoacetophenone conjugated skeleton except for the oxime phenyl group. The electron density of HOMO–LUMO transition showed the fluorophore-metal charge transfer, indicating that with the PET effect, the excited electrons were readily averted to metal ions (Cui et al. 2019; Li et al. 2021b). The decrease of

Table 1 Comparison of some recently reported probes for Zn^{2+} detection

Method	medium used	Detection limit(M)	Practical Test paper	Practical actual water	References
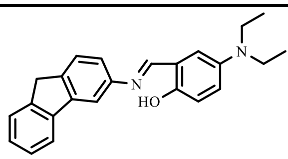	$MeCN:H_2O$ (V/V=19:1)	4.7×10^{-6}	-	Yes	Zhang et al. (2019)
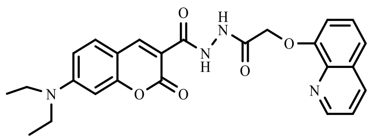	MeCN	6.00×10^{-7}	Yes	-	Kang et al. (2019)
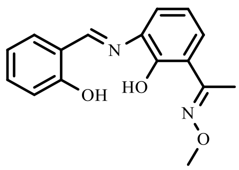	$MeOH/H_2O$ (V/V=9:1)	1.44×10^{-7}	-	-	Dong et al. (2017)
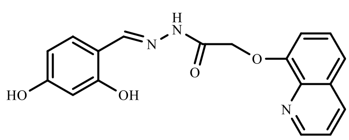	EtOH	3.50×10^{-7}	-	-	Fan et al. (2020)
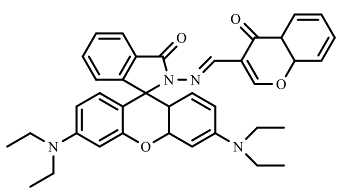	DMSO/EtOH (V/V=2:3)	1.34×10^{-7}	Yes	-	Xue et al. (2019)
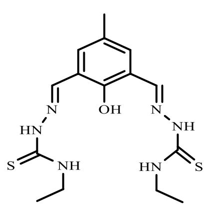	EtOH/HEPES (V/V=7:3)	3.35×10^{-7}		Yes	Purkait et al. (2019)
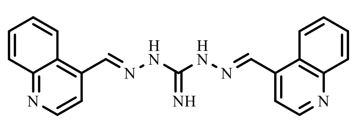	MeOH-tris buffer (v/v=1:1)	1.23×10^{-6}	-	Yes	Rout et al. (2019)
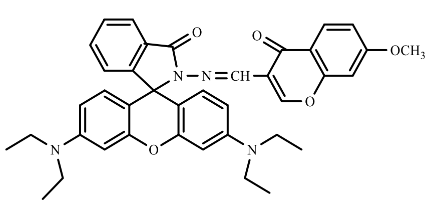	$MeOH/H_2O$ (V/V=1:1)	1.60×10^{-7}	-	-	Liu et al. (2018)
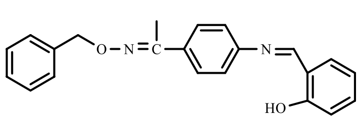	$DMSO/H_2O$ (V/V=9:1)	2.53×10^{-8}	Yes	Yes	This work

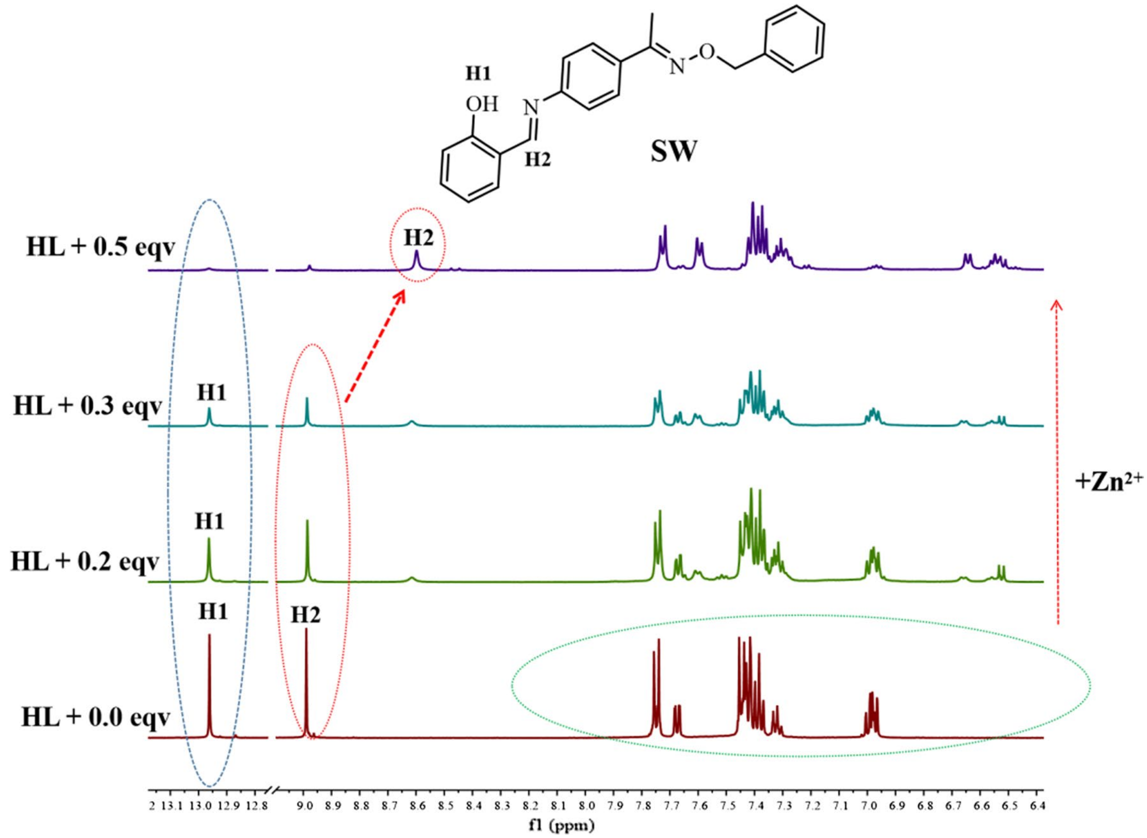

Fig. 4 [1]H NMR titration of SW with different concentrations of Zn^{2+} in d_6-DMSO

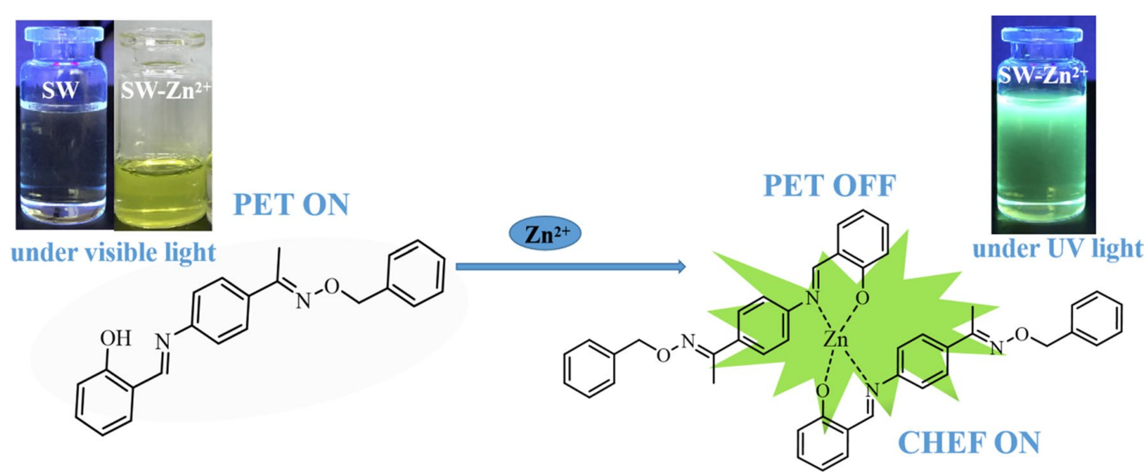

Scheme 2 Plausible mechanism for Zn^{2+} recognition by SW

ΔE indicates that there is good coordination ability between Zn^{2+} and SW and formed a stable environment.

Practical application of probe SW

In practical application, the probe SW is designed as a Zn^{2+} responsive strip sensor with good selectivity, and it can quickly and simply detect Zn^{2+} ions by changing the

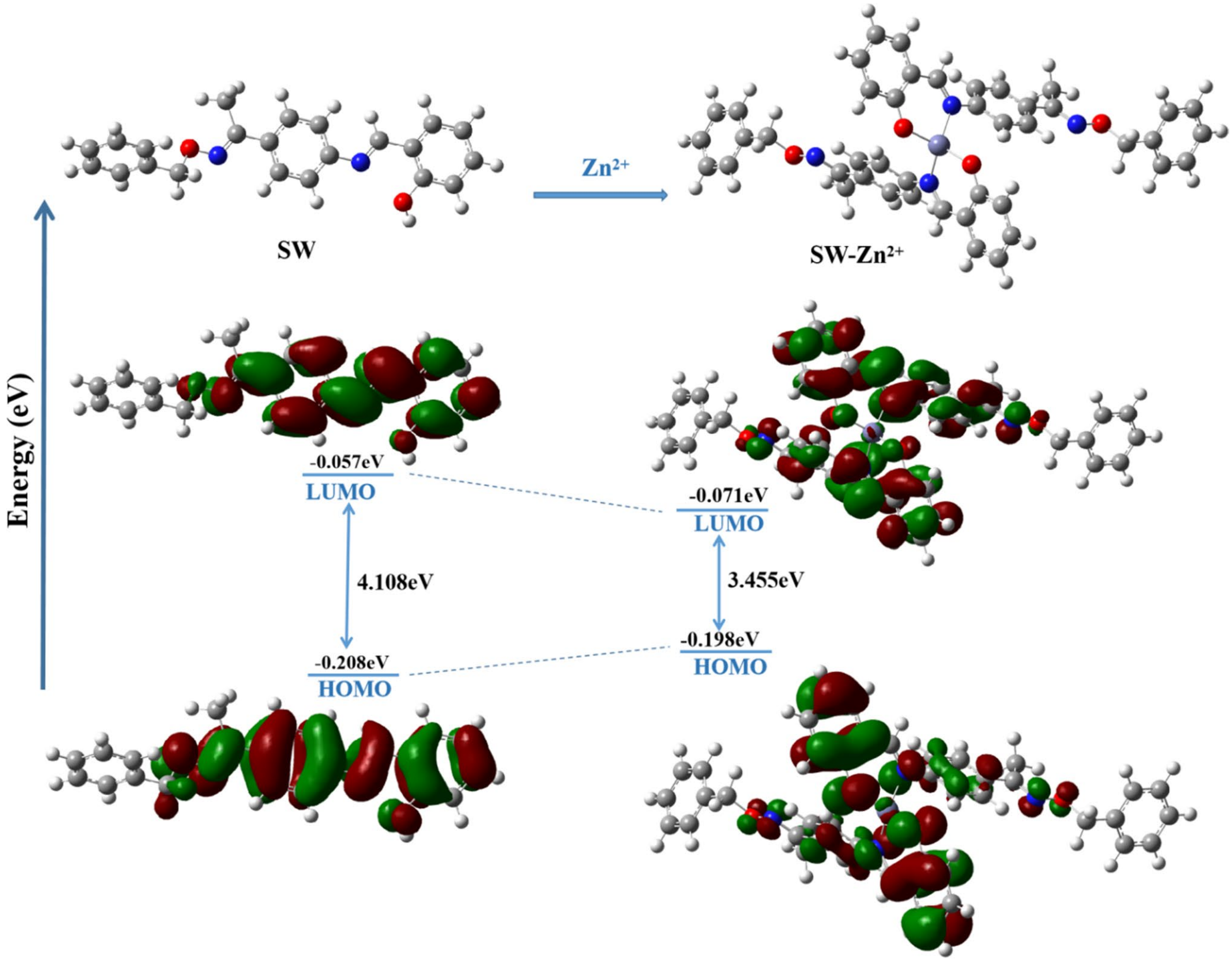

Fig. 5 optimization molecular structure of SW and SW-Zn^{2+}, molecular orbital diagrams of HOMO and LUMO

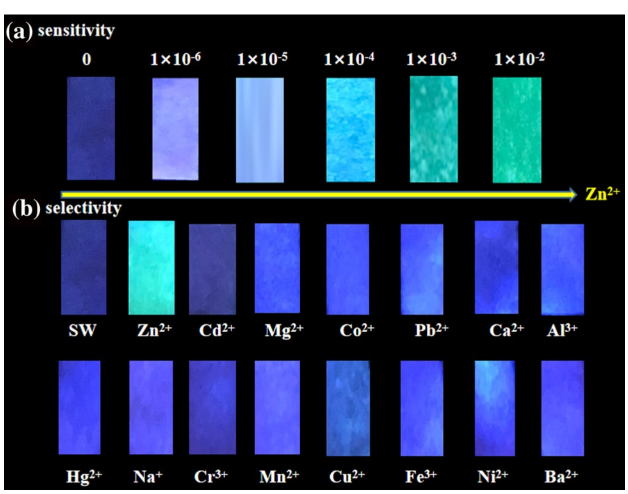

Fig. 6 Fluorescent tests paper of probe **SW**. **a** The changes after adding different concentrations of Zn^{2+} ions; **b** addition of different metal ions (1.0×10^{-2} mol/L)

wavelength, which has great practical value (Kang et al. 2019a). The filter strips were immersed in DMSO/H_2O solution of probe SW for 1 h, and dried at low temperature, then immersed in different concentrations of Zn^{2+} ions and other metal ions for 30 min, and the changes were observed under 365 nm UV lamps (Diao et al. 2018). As shown in Fig. 6a, with the increase of Zn^{2+} concentration, the color of the test paper changed from colorless to green. Whereas the other metal ions did not cause obvious changes in the color of test paper except Zn^{2+} ions (Fig. 6b), indicating that SW probe had high selectivity for Zn^{2+}.

In order to test the practicability of Zn^{2+} ions in real water samples, drinking water, tap water and Yellow River Water were collected for sensing experiments (Sarkar et al. 2020). All samples were filtered through 0.2 mm filter membrane and tested for three times. The calibration curve was obtained by measuring the Zn^{2+} ions concentration

Table 2 Determination of Zn^{2+} ions in actual water samples

Sample	Zn^{2+} added (μM)	Zn^{2+} found (μM)	Recovery (%)	R.S.D. (% n = 3)
Drinking water	5.0	5.01	100.2	0.32
	10.0	9.95	99.5	0.21
	15.0	14.82	98.8	1.52
Tap water	5.0	5.04	100.8	0.94
	10.0	10.11	101.1	1.81
	15.0	14.93	98.8	1.37
Yellow River Water	5.0	5.12	102.4	2.08
	10.0	9.98	99.8	0.89
	15.0	15.18	101.2	2.68

Conditions: probe SW = 20 μM in DMSO/H_2O solution (v/v = 9:1)

(Ke et al. 2020). As shown in Table 2, the detection results show that the probe SW can effectively detection Zn^{2+} ions and has high recovery (98%-103%), good analytical precision (RSD < 3%), which meets the detection requirements. Therefore, the probe SW can be effectively used for the detection of Zn^{2+} ion concentration in actual water samples and has practical value in environmental analysis.

Conclusions

In summary, a simple Schiff base ligand SW has been designed and synthesized, and it has higher sensitivity and selectivity to Zn^{2+} in DMSO/H_2O (v/v = 9:1) solution. And the detection limit of the SW to Zn^{2+} is down to 2.53×10^{-8} mol/L, which was lower than the limited value defined by WHO. By means of ^{1}H NMR, MS analysis and theoretical calculation, we obtained the binding mode of probe SW to Zn^{2+} is 2:1. In addition, the probe SW can be used for the detection of Zn^{2+} ions in the test paper under the UV light at 365 nm and the detection of Zn^{2+} ions in actual water samples, which has a potential application prospect.

Supplementary Information The online version contains supplementary material available at https://doi.org/10.1007/s11696-021-01684-x.

Acknowledgements This work was supported by the Science and Technology Program of Gansu Province (18YF1GA054) and the Program for Excellent Team of Scientific Research in Lanzhou Jiaotong University (201706), both of which are gratefully acknowledged.

Author Contributions All authors contributed to the study conception and design. Data collection and analysis were performed by all authors. The first draft of the manuscript was written by Juan Li and all authors commented on previous versions of the manuscript. All authors read and approved the final manuscript.

Funding This work was supported by the Science and Technology Program of Gansu Province (18YF1GA054) and the Program for the Excellent Team of Scientific Research in the Lanzhou Jiaotong University (201706).

Data Availability The data sets used and/or analyzed during the present study are available from the corresponding author on reasonable request.

Declaration

Conflicts of interest The authors declare that they have no conflict of interest.

References

Anand T, Ashok Kumar SK, Sahoo SK (2017) Vitamin B6 cofactor derivative: a dual fluorescent turn-on sensor to detect Zn2+ and CN− ions and its application in live cell imaging. Chem Select 2:7570–7579. https://doi.org/10.1002/slct.201701024

Anand T, Ashok Kumar SK, Sahoo SK (2018) A novel Schiff base derivative of pyridoxal for the optical sensing of Zn2+ and cysteine. Photochem Photobiol 17:414–422. https://doi.org/10.1039/C7PP00391A

Bian RN, Wang JF, Xu X, Dong WK, Ding YJ (2021) Investigation of mononuclear, dinuclear, and trinuclear transition metal (II) complexes derived from an asymmetric Salamo-based ligand possessing three different coordination modes. Appl Organomet Chem 35:e6040. https://doi.org/10.1002/aoc.6040

Bian RN, Xu X, Feng T, Dong WK (2021) A novel O-phenanthroline-based bis(half-salamo)-like chemical sensor: For rapid and efficient continuous recognition of Cu^{2+}, HPO_4^{2-} and $H_2PO_4^{-}$. Inorg Chim Acta 516:120098. https://doi.org/10.1016/j.ica.2020.120098

Chang J, Zhang SZ, Wu Y, Zhang HJ, Sun YX (2020) Three supramolecular trinuclear Nickel(II) complexes based on Salamo-type chelating ligand: Syntheses, crystal structures, solvent effect, Hirshfeld surface analysis and DFT calculation. Transit Met Chem 45:279–293. https://doi.org/10.1007/s11243-020-00379-8.26

Cui YF, Zhang Y, Xie KF, Dong WK (2019) A newly synthesized heterobimetallic Ni^{II}-Gd^{III} salamo-BDC-based coordination polymer: Structural characterization, DFT calculation, fluorescent and antibacterial properties. Crystals 9:596. http://creativecommons.org/licenses/by/4.0/.

Diao HP, Guo LX, Liu W, Feng LH (2018) A novel polymer probe for Zn(II) detection with ratiometric fluorescence signal. Spectrochim

Acta Part A 196:274–280. https://doi.org/10.1016/j.saa.2018.02.036

Dong WK, Akogun FS, Zhang Y, Sun YX, Dong XY (2017) A reversible "turn-on" fluorescent sensor for selective detection of Zn^{2+}. Sensor Actuat B 238:723–734. https://doi.org/10.1016/j.snb.2016.07.047

Fan L, Qin JC, Li CR, Yang ZY (2020) Two similar Schiff-base receptor based quinoline derivate: Highly selective fluorescent probe for Zn(II). Spectrochimica Acta Part A 236:118347. https://doi.org/10.1016/j.saa.2020.118347

Feng T, Li LL, Li YJ, Dong WK (2021) A half-salamo-based pyridine-containing ligand and its novel Ni^{II} complexes including different auxiliary ligands: Syntheses, structures, fluorescence properties, DFT calculations and Hirshfeld surface analysis. Acta Cryst B 77:168–181. https://doi.org/10.1107/S2052520620016157

Kang TT, Wang HP, Wang XJ, Feng LH (2019a) A facile Zn(II) probe based on intramolecular charge transfer with fluorescence red-shift. Microchem J 148:442–448. https://doi.org/10.1016/j.microc.2019.05.035

Kang T, Wang H, Wang X, Feng L (2019b) A facile Zn(II) probe based on intramolecular charge transfer with fluorescence red-shift. Microchem J 148:442–448. https://doi.org/10.1016/j.microc.2019.05.035

Ke HS, Wei W, Yang YS, Wu HP, Zhang YQ, Xie G, Chen SP (2020) A trinuclear zinc coordination cluster exhibiting fluorescence, colorimetric sensitivity, and recycling of silver ion and detection of cupric ion. Inorg Chem 21:24–39. https://doi.org/10.1021/acs.inorgchem.9b03169

Li YJ, Guo SZ, Feng T, Xie KF, Dong WK (2021) An investigation into three-dimensional octahedral multi-nuclear Ni(II)-based complexes supported by a more flexible salamo-type ligand. J Mol Struct 1228:129796. https://doi.org/10.1016/j.molstruc.2020.129796

Li P, Yao GX, Li M, Dong WK (2021) Influence of different counteranions on supramolecular self-assemblies, Hirshfeld surfaces analyses and fluorescence properties of three multinuclear Cu(II) salamo-based complexes. Polyhedron 195:114981. https://doi.org/10.1016/j.poly.2020.114981

Li RY, Wei ZL, Wang L, Zhang Y, Ru JX (2021) A new salamo-based fluorescence probe to visually detect aluminum(III) ion and bio-imaging in zebrafish. Microchem J 162:105720. https://doi.org/10.1016/j.microc.2020.105720

Liu LM, Yang ZY (2018) A rhodamine and chromone based "turn-on" fluorescent probe (RC1) for Zn(II) in aqueous solutions and its application. J Photoch Photobio A 364:558–563. https://doi.org/10.1016/j.jphotochem

Liu YJ, Qiu DL, Pan H, Li MG, Chen HB, Li HM (2018) A high selective fluorescent probe for colourimetric recognition of cyanide anion based on heptamethine cyaninetriphenylamine conjugate. J Photoch Photobio A 364:151–158. https://doi.org/10.1016/j.jphotochem.2018.06.018

Liu C, Wei ZL, Mu HR, Dong WK, Ding YJ (2020) A novel unsymmetric bis(salamo)-based chemosensor for detecting Cu^{2+} and continuous recognition of amino acids. J Photoch Photobio A 397:112569. https://doi.org/10.1016/j.jphotochem.2020.112569

Liu C, An XX, Cui YF, Xie KF, Dong WK (2020) Novel structurally characterized hetero-bimetallic $[Zn(II)_2M(II)]$ (M=Ca and Sr) bis(salamo)-type complexes: DFT calculation, Hirshfeld analyses, antimicrobial and fluorescent properties. Appl Organomet Chem 34:e5272. https://orcid.org/0000-0003-1249-5808.

Long RQ, Tang C, Yang Z, Fu QC, Xu JJ, Tong CY, Shi SY, Guo Y, Wang DJ (2020) Natural hyperoside based novel light-up fluorescent probe with AIE and ESIPT characteristics for on-site and long-term imaging of β-galactosidase in living cells. J Mater Chem C 00:1–5. https://doi.org/10.1039/D0TC01981J

Lu MM, Qiu SY, Cui SQ, Pu SZ (2020) A novel diarylethene-based fluorescence sensor with a benzohydrazide unit for the detection of Zn^{2+}. J Phys Org Cheme e:4113. doi: https://doi.org/10.1002/poc.4113.

Mu HR, Yu M, Wang L, Zhang Y, Ding YJ (2020) Catching S^{2-} and Cu^{2+} by a high sensitive and efficient salamo-like fluorescence-ultraviolet dual channel chemosensor. Phosphorus Sulfur 195:730–739. https://doi.org/10.1080/10426507.2020.1756807

Ozdemir M (2016) A selective fluorescent "turn-on" sensor for recognition of Zn^{2+} in aqueous media. Spectrochim Acta Part A 161:115–121. https://doi.org/10.1016/j.saa.2016.02.040

Pan YQ, Xu X, Zhang Y, Zhang Y, Dong W-K (2020) A high sensitive and selective bis(salamo)-type fluorescent chemosensor for identification of Cu^{2+} and the continuous recognition of S^{2-}. Spectrochim Acta Part A 229:117917–117921. https://doi.org/10.1016/j.saa.2019.117927

Pan YQ, Zhang Y, Yu M, Zhang Y, Wang L (2020) Newly synthesized homomul trinuclear Co(II) and Cu(II) bissalamo-like complexes: Structural characterizations, Hirshfeld analyses, fluorescence and antibacterial properties. Appl Organomet Chem 34:e5441. https://orcid.org/0000-0002-4806-2708.

Pannipara MB, Sehemi AG, Irfan A, Assiri M, Kalam A, Yahya S (2018) AIE active multianalyte fluorescent probe for the detection of Cu^{2+}, Ni^{2+} and Hg^{2+} ions. Spectrochim Acta Part A 201:54–60. https://doi.org/10.1016/j.saa.2018.04.052

Patil M, Keshav K, Kumawa M, Bothra S, Sahoo SK, Srivastava R, Rajput J, Bendre R, Kuwar A (2018) Monoterpenoid derivative based ratiometric fluorescent chemosensor for bioimaging and intracellular detection of Zn^{2+} and Mg^{2+} ions. J Photoch Photobio A 364:758–763. https://doi.org/10.1016/j.jphotochem.2018.07.015

Purkait R, Mahapatra AD, Chattopadhyay D, Sinha C (2019) An azine-based carbothioamide chemosensor for selective and sensitive turn-on-off sequential detection of Zn(II) and $H_2PO_4^-$, live cell imaging and INHIBIT logic gate. Spectrochim Acta A 207:164–172. https://doi.org/10.1016/j.saa.2018.09.019

Rout K, Manna AK, Sahu M, Patra GK (2019) A guanidine based bis Schiff base chemosensor for colorimetric detection of Hg(II) and fluorescent detection of Zn(II) ions. Inorg Chim Acta 486:733–741. https://doi.org/10.1016/j.ica.2018.11.021

Sarkar A, Aratrika C, Tonmoy C, Suranjana P, Debabrata S, Suvendu M, Debasis D (2020) A chemodosimetric approach for fluorimetric detection of Hg2+ ions by trinuclear Zn(II)/Cd(II) schiff base complex: first case of intermediate trapping in a chemodosimetric approach. Inorg Chem 12:30–52. https://doi.org/10.1021/acs.inorgchem.0c00857

Sudipa M, Santi MM, Durbadal O, Debprasad C, Chittaranjan S (2019) Water soluble sulfaguanidine based Schiff base as a "Turn-on" fluorescent probe for intracellular recognition of Zn^{2+} in living cells and exploration for biological activities. Polyhedron 172:28–38. https://doi.org/10.1016/j.poly.2019.02.042

Sun YX, Lu RE, Li XR, Zhao YY, Li CY (2015) Synthesis and Supramolecular Structure of Ligands Containing Oxime Group Schiff Base and Cu(II) Complexes. Chinese J Inorg Chem 31:1055–1062. https://doi.org/10.11862/CJIC.2015.134

Sun YX, Pan YQ, Xu X, Zhang Y (2019) Unprecedented dinuclear Cu(II) N,O-donor complex: Synthesis, structural characterization, fluorescence property, and hirshfeld analysis. Crystals 9:607. https://doi.org/10.3390/cryst.9120607

Upadhyay Y, Anand T, Babu LT, Paira P, Crisponi C, Ashok Kumar SK, Kumar R, Sahoo SK (2018) Three-in-one type fluorescent sensor based on a pyrene pyridoxal cascade for the selective detection of Zn(II), hydrogen phosphate and cysteine. Dalton T 47:742. https://doi.org/10.1039/C7DT04234E

Vetriarasu V, Selva Kumar R, Ashok Kumar SK, Sahoo SK (2019) Highly selective turn-on fluorogenic chemosensor for Zn^{2+} based on chelation enhanced fluorescence. Inorg Chem Commun 102:171–179. https://doi.org/10.1016/j.inoche.2019.02.020

Wang JL, Hao YF, Wang H, Yang SX, Tian HY, Sun BG, Liu YG (2017) Rapidly responsive and high selective fluorescent probe for bisulfite detection in food. J Agric Food Chem 65:2883–2887. https://doi.org/10.1021/acs.jafc.7b00353

Wang L, Wei ZL, Liu C, Dong WK, Ru JX (2020) Synthesis and characterization for a high selective bis(salamo)-based chemical sensor and imaging in living cell. Spectrochim Acta A 239:118496. https://doi.org/10.1016/j.saa.2020.118496

Wang L, Wei ZL, Chen ZZ, Liu C, Dong WK, Ding YJ (2020) A chemical probe capable for fluorescent and colorimetric detection to Cu^{2+} and CN^- based on coordination and nucleophilic addition mechanism. Microchem J 155:104801. https://doi.org/10.1016/j.microc.2020.104801

Wang B, Liu X, Duan W, Dai S, Lu H (2020) Visual and ratiometric fluorescent determination of Al^{3+} by a red-emission carbon dot-quercetin system. Microchem J 156:104807. https://doi.org/10.1016/j.microc.2020.104807

Wang L, Pan YQ, Wang JF, Zhang Y, Ding YJ (2020a) A high selective and sensitive half-salamo-based fluorescent chemosensor for sequential detection of Pb(II) ion and Cys. J Photochem Photobio A 400:112719. https://doi.org/10.1016/j.jphotochem.2020.112719

Wang JF, Feng T, Li YJ, Sun YX, Dong WK, Ding YJ (2021) Novel structurally characterized Co(II) metal-organic framework and Cd(II) coordination polymer self-assembled from a pyridine-terminal salamo-like ligand bearing various coordination modes. J Mol Struct 1231:129950. https://doi.org/10.1016/j.molstruc.2021.129950

Wang JF, Bian RN, Feng T, Xie KF, Wang L, Ding YJ (2021) A highly sensitive dual-channel chemical sensor for selective identification of $B_4O_7^{2-}$. Microchem J 160:105676. https://doi.org/10.1016/j.microc.2020.105676

Wei ZL, Wang L, Wang JF, Guo WT, Zhang Y, Dong WK (2020) Two high sensitive and efficient salamo-like copper (II) complex probes for recognition of CN^-. Spectrochim Acta Part A 228:1386–1425. https://doi.org/10.1016/j.saa.2019.117775

Wu Y, Ding WM, Li J, Guo G, Zhang SZ, Jia HR, Sun YX (2021) A Highly selective turn-on fluorescent and naked-eye colorimetric dual-channel probe for cyanide anions detection in water samples. J Fluoresc 31:437–446. https://doi.org/10.1007/s10895-020-02677-x

Xu X, Bian RN, Guo SZ, Dong WK, Ding YJ (2020) A new asymmetric salamo-based chemical sensor for dual channel detection of Cu^{2+} and $B_4O_7^{2-}$. Inorg Chim Acta 513:119945. https://doi.org/10.1016/j.ica.2020.119945

Xu X, Li YJ, Feng T, Dong WK, Ding YJ (2021) Highly efficient detection of Cu^{2+} and $B_4O_7^{2-}$ based on a recyclable asymmetric salamo-based probe in aqueous medium. Luminescence 36:169–179. https://doi.org/10.1002/bio.3932

Xu X, Feng T, Feng SS, Dong WK (2021) Influence of structural variation of salamo-based ligand on supramolecular architectures, Hirshfeld analyses, and fluorescence properties of new tetranuclear Ni^{II} complexes. Appl Organomet Chem 35:e6057. https://doi.org/10.1002/aoc.6057

Xue J, Tian LM, Yang ZY (2019) A novel rhodamine-chromone Schiff-base as turn-on fluorescent probe for the detection of Zn(II) and Fe(III) in different solutions. J Photochem Photobio A 369:77–84. https://doi.org/10.1016/j.jphotochem

Yu B, Sun YX, Yang CJ, Guo JQ, Li J (2017) Synthesis and crystal structures of an unexpected tetranuclear Zinc(II) complex and a benzoquinone compound derived from Zn^{2+} and Cd(II)-promoted reactivity of schiff base ligands. Z Anorg Allg Chem 643:689–698. https://doi.org/10.1002/zaac.201700034

Yu B, Li CY, Sun YX, Jia HR, Guo JQ, Li J (2017) A new azine derivative colourimetric and fluorescent dual-channel probe for cyanide detection. Spectrochim Acta Part A 184:249–254. https://doi.org/10.1016/j.saa.2017.05.012

Zhang HJ, Chang J, Jia HR, Sun YX (2018) Syntheses, supramolecular structures and spectroscopic properties of Cu(II) and Ni(II) complexes with Schiff base containing oxime group. Chinese J Inorg Chem 34:2261–2270. https://doi.org/10.11862/CJIC.2018.261

Zhang JZ, Zhao Z, Shang H, Liu QS, Liu F (2019) An easy-to-synthesize multi-photoresponse smart sensor for fast detecting Zn^{2+} and quantifying Fe^{3+} based on the enol/keto binding mode. New J Chem 11(58):54. https://doi.org/10.1039/C9NJ03635K

Zhang SZ, Chang J, Zhang HJ, Sun YX, Wu Y, Wang Y-B (2020) Synthesis, crystal structure and spectral properties of binuclear Ni(II) and cubane-like Cu4(μ3-O)4 Cored Tetranuclear Cu(II) complexes based on coumarin schiff base. Chinese J Inorg Chem 36:503–514. https://doi.org/10.11862/CJIC.2020.056

Zhang SZ, Guo G, Ding WM, Li J, Wu Y, Sun YX (2021) Synthesis and spectroscopic properties of two different structural Schiff base Zn(II) complexes constructed with/without auxiliary ligands. J Mol Struct 1230:129627. https://doi.org/10.1016/j.molstruc.2020.129627

Zhao Q, An XX, Liu LZ, Dong WK (2019) Syntheses, luminescences and Hirshfeld surfaces analyses of structurally characterized homo-trinuclear Zn^{2+} and hetero-pentanuclear Zn^{2+}-Ln^{III} (Ln=Eu, Nd) bis(salamo)-like complexes. Inorg Chim Acta 490:6–15. https://doi.org/10.1016/j.ica.2019.02.040.38